Objective Quantification of Circular Vection in Immersive Environments

Debadutta Subudhi[(✉)] , P. Balaji , and Manivannan Muniyandi

Touch Lab, Department Applied Mechanics, Indian Institute of Technology Madras, Chennai 600 113, India
dev.subudhi49@gmail.com, mani@iitm.ac.in

Abstract. Human interaction in the computer environment requires conduciveness with minimal cybersickness. One such sickness is vection, where the subjects undergo illusory perception of self-motion in response to visual stimulus. The present research quantifies the perceptual parameter. An optokinetic drum (OKD) is used to induce circular vection on a virtual reality (VR), and the inertial measurement unit (IMU) in a head-mounted display (HMD) is used to track the head rotation about x, y, z axes. The study quantifies the vection in terms of the vection index (VI). The VI depends on the ratio of the angular velocity of HMD to the angular velocity of OKD. There is a significant difference from resting state to higher angular speeds in clockwise (CW) as well as anticlockwise (ACW) direction ($p < 0.05$). Also, the circular vection along the y-axis imparts the motion along the x and z axes. The magnitude of vection increases with speed in CW and ACW directions till the optimum speed of OKD. The vection is absent during very low and high speeds of OKD. Most participants experience the self-motion in an angular displacement range of 30–97°/s in both CW and ACW directions. The vection in ACW compensates for the vection in CW direction about x, y and z axes.

Keywords: Motion sickness · OKD · VI · IMU

1 Introduction

Motion sickness (MS) is a general experience of discomposure in response to motion stimuli present in a real or virtual environment. The MS depends on the ocular and vestibular organs that sense the motion and stabilize the gaze in real-world through vestibulo-ocular reflex (VOR) [19]. However, in a virtual environment, motion sickness is predominantly visually induced, known as visually induced motion sickness (VIMS). According to the Ebenholtz hypothesis, exposing individuals to various visual movements causes VIMS [16]. The VIMS depends on several factors, such as the conflict in VOR and somatosensory graviceptor[11] inputs. The magnitude of the phase difference between these sensory inputs causes a higher probability of VIMS [49].The other reasons of VIMS

---

are optokinetic nystagmus (OKN) [15] and body posture disability [51]. Conflict in VOR is effectively perceived by humans [5]. Researchers create vestibulo-ocular conflict by a rotating chair [61], flow field video [57], an off-vertical axis [9], a parallel swing [65], and a driving simulator [35], to trigger the vestibular system. However, the VIMS depends on eye movement in different directions, saccades and eye blinks [10]. The effect of VIMS on the eye leads to minor postural changes in the head that transmits to the semicircular canal sensing the changes in angular velocity of the head. This oculo-vestibular reflex (OVR) is not explored in literature.

1.1   Vection

The vection is an illusory perception of self-motion in real and virtual immersive environments. The nature of vection can be circular, linear or a combination of linear and circular. The OKD is a general apparatus used to discover many properties of perception of self-motion [1,29,47]. Different input modalities can induce vection, such as auditory-induced vection (AIV) [33], Hapto-kinetic Vection (HKV) is induced by applying tactile motion on the body [14,42], Biomedical vection (BMV) is induced from treadmill motion [7,52], visually induced vection (VIV) from computer display [64] by OVR. The intensity of vection depends on the flow, and apparent depth of the objects in the visual field [40]. It also depends on the time of exposure, and literature shows that a visual stimulus for 10 s is enough to induce illusory self-motion [14]. Also, the characterization of vection depends on which part of the body perceives self-motion. Most subjects experience VIMS reported vection; however, VIMS can happen in the dearth of vection [38]. The vection in virtual environments deteriorates the immersion. Therefore, nullifying the cause of vection is primary for the design of most of the head-mounted displays (HMD). It requires objectification and measurement of vection in VR.

1.2   Vection Measurement Methods

There is both subjective and objective measurement of vection in literature. However, the objective measurements are more effective in vection quantification compared to subjective measurements [44] as it aids in control and validation. Yet, the subjective measurements provide an insight towards the parameters resulting in self-motion. Subjective measure reports onset/offset of self-motion and it's strength from joystick button [20], rotation of circular knob in response to spinning OKD at 0.1—100 °/s² in real environment[41] or in VR [37], magnitude estimation (ME) ratings on a 10 or 100-point scale [2,8,36,46]. Eye movement and eccentric gaze conditions also objectify the vection strength at slower eye velocity [34]. The alpha power in electroencephalogram (EEG) during spatial disorientation due to vection increases variably among the subjects [58]. Other objective parameters such as heart rate (HR), blood pressure (BP) and skin conductance level (SCL) measures vection [10]. There is greater variability among subjects due to vestibular and somatosensory control of the autonomic nervous system while

quantifying vection [3]. The literature shows the neural response of vection from positron emission tomography(PET) [13], Magnetoencephalography (MEG) [63], and functional magnetic resonance imaging (fMRI) [54].

Measurement of Vection from EEG: EEG is independent of subjective response and has a higher temporal resolution in the order of milliseconds and can sense the vection from time-frequency analyses of event-related brain potentials (ERP) [32]. There is an increase 10 Hz alpha wave activity at 14 s followed by a decrease in beta and delta activity as the ten participants subjected to linear vection with two types of optic flow display, which constitutes of 1000 blue circular dots of $0.36°$ in diameter moving at a 1 m/s on a black background [45]. Studies show that negative inflection $N230$ at O_1 (left occipital), and O_2 (right occipital) is more pronounced to visual stimuli producing stronger vection during longer 45 s stimulus exposure [31]. Literature also suggests that the EEG may be informative about inducing potential towards vection by optic flow. At the same time, stimulus exposure of 2.5–3.5 s is minimal to cause vection during EEG recording [45]. EEG can indicate cortical processing towards vection onset or offset and magnitude of vection. However, EEG measures can reflect parameters that are not purely vection-related [32].

Measurement of Vection from EGG: Vection causes an increase in gastric tachyarrhythmia, an increase in sympathetic activity, and a decrease in parasympathetic activity. Exposure to the virtual environment through OKD causes more stomach contraction activity [24]. Optokinetic stimulation causes a rise in frequency of EGG from 3.0 cycles/min to "tachygastric" frequencies (4–9) cycles/min [56]. However, various research studies scored tachygastric condition differently [55].

Measurement of Vection from EOG: The EOG parameters from the eye tracker in a few HMDs, such as the number of eye blinks, eye movement, pupil diameter and pupil position, are some factors showing the level of vection in VR. The mean eye blinking rate (number/min) is lower in the initial minutes of visual stimulus exposure, and it is considerably higher during the middle of the trials [35]. The blinking rate per epoch is more in HMD than display monitor [12]. Also, the foveal retinal slip velocity is an essential parameter towards the level of VIMS [21]. However, some studies in OKD rotation claims that unnatural and random eye motion can distort VIMS and eye fixation can nullify the effect of it [28,56,67].

Measurement of Vection from SCL: Skin conductance level is the tonic part of electrodermal activity (EDA), responsible for autonomic changes in the electrical conductance of the skin. It depends on autonomic arousal due to emotional and cognition loads. Compared to the baseline, SCL is high during the final minutes of experience in VR using the driving simulator as well as OKD

rotation [35]. The OKD rotating at 60^0 per second (10 cycles per minute (cpm)) for 12 min causes an increase in both tonic and phasic levels at both palm and forehead sites (sensitive) with a positive Pearson correlation coefficient of 0.62 at forehead site than 0.48 at palmer site [59].

Measurement of Vection from Heart Rate Variability(HRV), BP and Breath Rate (BR): The HRV provides a measure for the autonomic nervous system activity [6]. Most of the study shows that vection causes a higher heart rate of 1.54 Hz [26]during OKD simulator [23,66] with higher low frequency (0.04–0.15 Hz) power in the RR-interval, which results in higher sympathetic outflow during computer graphics (CG) and real roller coaster movie scene [62]. BP shows an upward trend when subjects are VR driving simulators [39] and OKD simulator[23]. Oscillatory scenes in displays play a significant role in enhancing the BP as well as BR [22] to 0.365 Hz [26].

1.3   Gaps in the Measurements of Vection and Present Research

The assessment of vection through methods in the literature is cumbersome from a practical point of view. These methods require additional hardware that might reduce immersion which is the main objective of VR systems. Therefore, the current study focuses on measuring the vection through elegant and straightforward methods without requiring additional hardware. The current research proposes that mild head movements can be recorded from IMUs in most HMDs. The authors propose a novel parameter, Vection Index (VI), for measuring the vection from the IMU data. The objective of the study is to quantify circular vection from the kinematic analysis of OKD and HMD. The hypothesis is that the drum velocity reflects in head velocity. The authors also emphasise perceiving the self-motion to the direction of drum rotation.

2   Method

2.1   Participants

A total of 18 postgraduate students ($Mean_{AGE} = 26, SD_{AGE} = 4.2$) $Mean_{Weight} = 76$ Kg, $SD_{weight} = 22.6$ kg participate in the study. One participant did not participate in the experiment because of slight nausea, leaving 17 participants (11 male, six female) in the final analysis. There is no history of vestibular disorders among the participants, and they report the display is clear.

2.2   Apparatus

An Oculus Quest-2 VR headset has a horizontal field of view of $89°$ and a vertical field of view of $93°$. The refresh rate 60 Hz. The virtual environment simulates the OKD with a 200 cm diameter. The camera viewpoint is 100 cm away from the inner surface of the OKD [37]. Each stripe in OKD has a width of 49.1 cm.

The width is kept wider than 33 cm [37] to avoid spatial convergence at higher angular velocity. The VR headset is set with an inter-ocular distance (IOD) of 64 mm for all participants [37]. To confirm that the participants perceive the interior of OKD, they are asked about the stimulus appearance as flat, convex, or concave at the beginning of the experiment. All participants observe the drum in a concave shape in game mode. The subjective measurement for the participants is about the perception of self-motion during CW and ACW directions of virtual drum rotation at the end of the experiment.

2.3 Stimuli

The OKD for graphical display is built in Unreal Engine 4.8. The vertical stripe pattern in the VR display moves with six speeds in CW and ACW directions. The experiment runs on a computer with an Intel Core i7 processor,3.6GH, NVIDIA GeForce GTX980ti graphics card and 32 GB RAM.

2.4 Design

The experiment has six drum speed from slow to fast angular velocity in CW and ACW directions ($0°/s$, $5°/s$, $30°/s$, $70°/s$, $97°/s$, $110°/s$, $115°/s$, $0°/s$, $–5°/s$, $–30°/s$, $–70°/s$, $–97°/s$, $–110°/s$, $–115°/s$, $0°/s$) constituting 14 experimental conditions with 14 time intervals. Each time interval lapses for 16 s which is close to the mean vestibular adaptation time constant during perception of real rotation [53]. The total duration of the experiment is 240 s. The subjects go through a trial before the experiment to familiarise the participants with the VR environment. The angular velocities follow a fourth-order logistic function (Sigmoid function) to mimic the naturally occurring events as shown in Fig. 1a. The angular acceleration is shown in Fig. 1b.
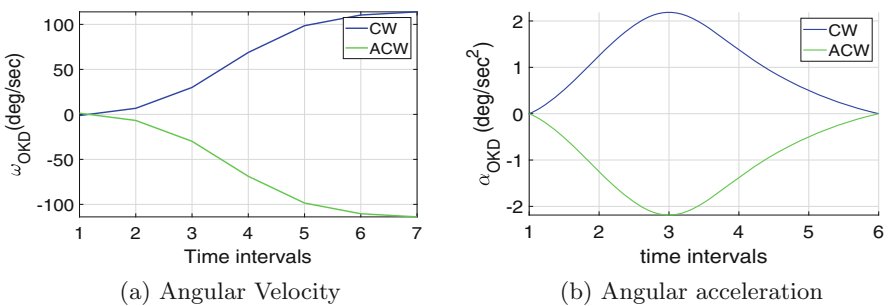

(a) Angular Velocity   (b) Angular acceleration

Fig. 1. Input angular velocity and acceleration from the OKD in VR fixed throughout the experiment

The authors define Vection Index (VI) as ratio of input angular velocity from virtual drum (ω_{OKD}) to angular velocity of HMD (ω_{HMD}) as shown in following

equations.

$$VI_{x,y,z} = \frac{[\omega_{OKD}]_y}{[\omega_{HMD}]_{x,y,z}} \tag{1}$$

$$VI = \sqrt{VI_x^2 + VI_y^2 + VI_z^2} \tag{2}$$

2.5   Procedure

Participants are seated upright on a grounded wooden chair in a dark room with their feet on the ground and heads unconstrained. Once participants are seated, the display is adjusted with 'Guardian' in the oculus-VR headset to get it in front of them. The participants are positioned at the centre of the virtual OKD by the camera setting. Participants go through one practice trial to get comfortable with the VR headset, stimulus, and task. The experiment begins with OKD starting from zero angular velocity in CW and ACW directions. The experimental setup is shown in Fig. 2.
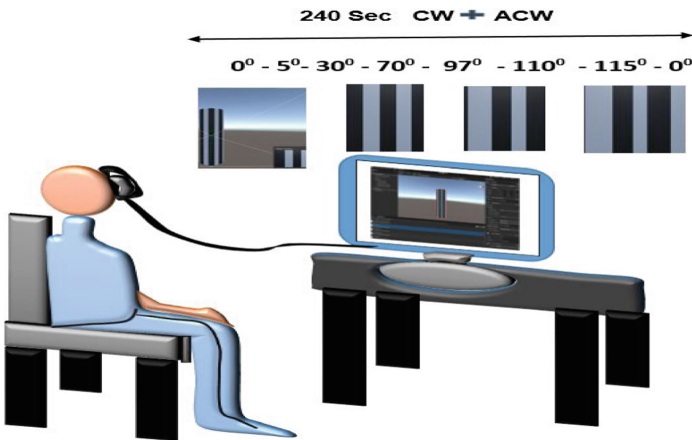

Fig. 2. Experimental set up showing various angular speeds of the virtual drum in both CW and ACW direction with head being unconstrained with body being grounded. The vertical stripes are for slow, medium and higher angular velocities.

3   Results

The vection strength is quantified from the angular displacement of HMD about X, Y, Z axes, which provides respective angular velocity and angular acceleration of HMD. The positional analysis is neglected as the stimulus here is rotational in nature. The t-test with 95% confidence intervals [27] is used to find the significant difference between different angular velocities.

3.1   Angular Displacement

The angular displacement of HMD for 16 s for a particular subject at each angular velocity of OKD is shown in Fig. 3. At zero angular velocity of OKD, the angular velocity of HMD has some flutters as the head can not be absolutely still. The head flutters get streamlined at lower speeds of OKD.
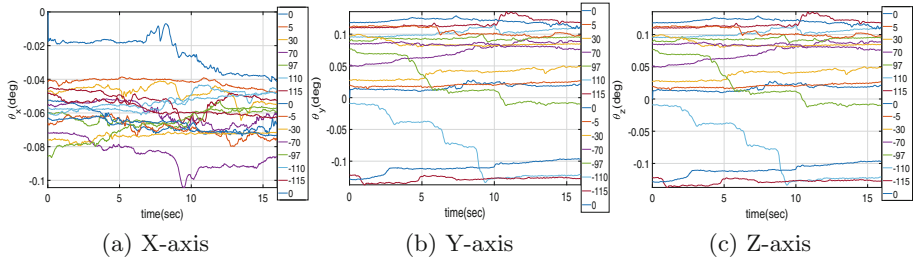

(a) X-axis   (b) Y-axis   (c) Z-axis

Fig. 3. Angular displacements$(\theta_x, \theta_y, \theta_z)$ of HMD for a typical sybject at various speed of OKD

The box plot of the angular displacements in Fig. 4 shows that the rotation of HMD about the y-axis follows a similar pattern of the inherent y-axis rotation of OKD. Also, the stimulus imparts rotation magnitude about other axes increase or decrease monotonously due to vection and weight of the HMD. There is a significant difference $p < 0.05$ between angular displacements at $70\,°/s$ in CW and $97\,°/s$, $110\,°/s$ in ACW than other angular velocities.

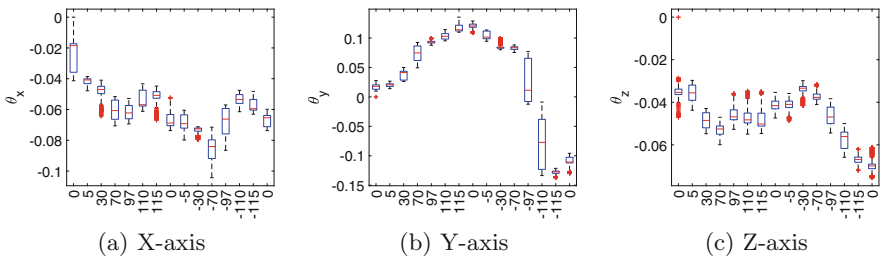(a) X-axis   (b) Y-axis   (c) Z-axis

Fig. 4. Box-plot of angular displacement for a typical subject considering various speeds of OKD about a. X-axis, b. Y-axis, c. Z-axis

3.2   Angular Velocity and Acceleration

The angular velocity is obtained by differentiating angular displacement of HMD with respect to a time interval, which is shown in Fig. 5.a. The angular velocity

of HMD increases as the speed of the virtual drum rises and decreases after reaching an optimal value in both CW and ACW directions of the drum about the y-axis of HMD than other axes. The peak value of the angular velocity of HMD about the y-axis occurs at $46\,°/$s in CW and $70\,°/$s in ACW direction.

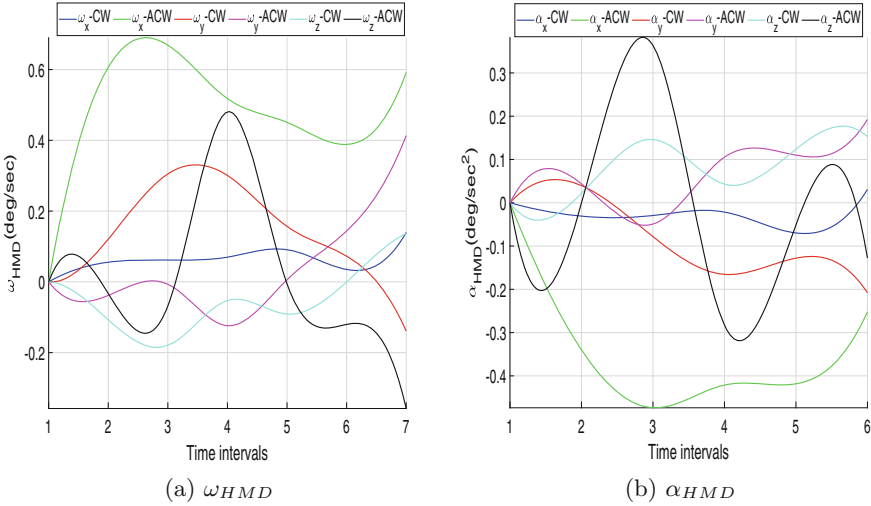(a) ω_{HMD} (b) α_{HMD}

Fig. 5. a. Scaled median angular velocity (Scaling factor of 10^3) about X,Y,Z axes in both CW and ACW directions of HMD for all subjects b. Scaled median angular acceleration (scaling factor of 10^4) about X,Y,Z axes in both CW and ACW directions of HMD considering all subjects.

The angular acceleration is obtained by differentiating the angular velocity of HMD with respect to a time interval, which is shown in Fig. 5.b. The angular acceleration of HMD increases uniformly after $30\,°/$s of ω_{OKD} about the y-axis signifying that the vection happens after a speed of $30\,°/$s.

3.3   Vection Index

The intensity of HMD motion increases as the speed of OKD increases. However, the vection happens at the acceleration of the drum (maximum slope region of the sigmoid (Fig. 1). The vection index follows the sigmoidal input velocity pattern of OKD (Fig. 6b). At very low and high speeds, the participants do not show vection. The perception of self-motion has lower and upper bound from 30–$97\,°/$s. However, the slope of the sigmoid for CW and ACW direction HMD is 0.5147 and 0.5138, respectively. This reflects in response from participants as most of the participants (47%) perceive vection in CW direction than in ACW direction as shown in Fig. 6c. This is the response for the sigmoidal input velocity of OKD, which is fixed throughout the experiments and has a slope of 0.5938 for both CW and ACW directions as shown in Fig. 1.
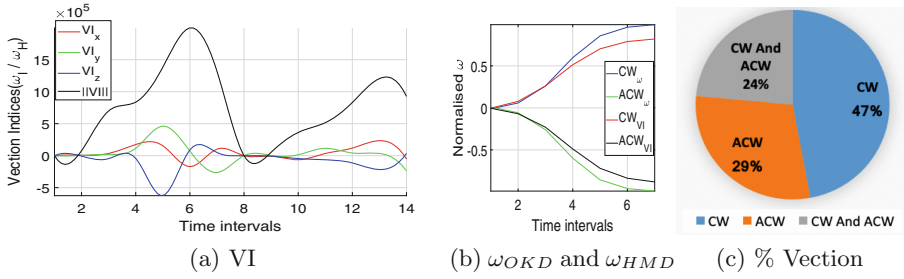
Fig. 6. a. Vection indices about x, y, z axes and magnitude of vection with a scaling factor of 0.001 for number of experimental conditions in x-axis, b. Normalised angular velocity of OKD and VI, c. Percentage of participants getting vection for different direction of motion pattern of OKD as in (b).

4   Discussion

4.1   Kinematic Analysis

The current paper has used the OKD to induce vection in an immersive VR environment and IMU readings from HMD as a method to quantify circular vection speed. However, the vection speed and strength is more complex since it involves multi-sensory inputs apart from visual input.

The kinematics of the HMD accurately depicts vection on the display's y-axis, and the impact may also be observed on other axes, albeit not as prominently as on the y-axis. The rate of change of angular velocity determines the vection strength, which is represented in the ω_y of HMD (CW_y, ACW_y) as in Fig. 5a, which mimics the angular acceleration of OKD (Fig. 1b). It may be due to the absence of vection at very low and high speeds of OKD and ω_y of HMD reaches a maximum magnitude close to maximum acceleration of OKD.

In contrast to the literature, which shows that vection is proportional to display speeds [41,43,47], the finding that the VI may have a derivative relationship with the motion of OKD is surprising. However, as evidenced by the current study, this is not always the case. Furthermore, greater speeds obscure peripheral vision, lowering vection since peripheral vision affects vection while central vision affects motion sickness, according to [61].

4.2   Vection Index

In both CW and ACW directions, VI is proportional to OKD speed. In Fig. 6b the current study reveals that the slope of the magnitude of the VI is smaller in the ACW direction than in the CW direction. As seen in Fig. 6a, the vection strength in the ACW compensates for the vection strength in the CW direction. This might be reversed if the OKD rotation starts with ACW and then CW. The study shows that the vection strength in ACW compensates for the vection strength in the CW direction as in. This could be reversed if rotaion of OKD

starts with ACW followed by CW. The pi-chart in Fig. 6c indicates a similar finding, with 47% of participants perceiving vection during CW rotation than ACW rotation, as seen by the slope of normalized-VI magnitude, which is larger for CW rotation. In contrary to the literature, where the vection speed from turning knob is higher than the speed of OKD [37], the slope of normalized-VI is lower than the slope of the OKD. This might be due to the fact that the knob is operated by hand, and during vection, skin conductance activity is greater at the palm location, but during the evaluation of vection via an HMD, the visual information travels through a complicated neural pathway, dampening head motion.

Moreover, in this study, the authors found that vection may occur in axes other than the Y-axis, such as X and Z, which are not the axes of rotation of the OKD (Y-axis), and that the weight of the HMD is a major contributor. As a result, the authors assess vection magnitude in terms of VI, considering motion across all axes. There is compensatory activity taking place to eliminate vection between axes. For example, in CW, vection about the y-axis is more than vection about the x and z axes in the CW direction, whereas in ACW, vection about the y-axis is less than vection about the x and z axes in the ACW direction.

The current work is unique in that the data are taken directly from the HMD, which will aid in forecasting vection speed and likely occurrence time in a dynamic scenario in diverse media such as water [18] or space. In essence, the slope of the vection index on a normalised scale is equivalent to the slope of display speed. Other research investigations have shown the same thing, albeit with various stimuli and measurements: vection speed is similar to display speed. In dynamic situations, further study is needed to determine the transfer function between display and vection indices, as well as a mathematical model.

5   Conclusion

The current study proposes a simple method of measuring the vection without requiring additional hardware. It shows that mild head movements can be recorded from IMUs in most HMDs. The study finds that vection intensity depends on the specific range of visual display motion and slope of the motion. The head response because of vection is a differential operator on the display acceleration. The vection is relatively dependent of the axis of rotation of the visual field, and it has a cross balancing property about other axes of rotation of HMD. The study proposes a novel parameter Vection Index (VI) from which vection intensity can be found in the dynamic virtual environments. The link between VI and display speed has practical implications for applications such as all types of motion simulation in air, water, space. Several sensory cues such as audio, smell, and tactile input from the environment enhance the realism, hence play a role in affecting VI due to sensory mismatches in simulators [4,17,25,30,48,50,60]. The VI can better aid in calibrating display speeds to auditory and vestibular cueing speeds in motion simulators and games. The multi-sensory effects on vection can be filtered with help of VI and can help in enhancing the immersion.

In this study the subjects are seated with motion of head alone. The body movements during standing or walking while navigating VR might distort the VI and the accuracy of vection detection may be erroneous. Future study could involve subjects with unconstrained body movements.

References

1. Aitken, J.: 2. On a new variety of ocular spectrum. Proc. Royal Soc. Edinburgh **10**, 40–44 (1880)
2. Allison, R.S., Zacher, J.E., Kirollos, R., Guterman, P.S., Palmisano, S.: Perception of smooth and perturbed vection in short-duration microgravity. Exp. Brain Res. **223**(4), 479–487 (2012)
3. Aoki, M., Thilo, K.V., Burchill, P., Golding, J.F., Gresty, M.A.: Autonomic response to real versus illusory motion (vection). Clin. Auton. Res. **10**(1), 23–28 (2000)
4. Aykent, B., Merienne, F., Guillet, C., Paillot, D., Kemeny, A.: Motion sickness evaluation and comparison for a static driving simulator and a dynamic driving simulator. Proc. Inst. Mech. Eng. Part D J. Autom. Eng. **228**(7), 818–829 (2014)
5. Barnett-Cowan, M., Harris, L.: Perception of simultaneity and temporal order of active and passive head movements paired with visual, auditory and tactile stimuli. In: 9th International Multisensory Research Forum (IMRF 2008), p. 168 (2008)
6. Berntson, G.G., et al.: Heart rate variability: origins, methods, and interpretive caveats. Psychophysiology **34**(6), 623–648 (1997)
7. Bles, W.: Stepping around circular vection and coriolis effects. In: Attention and Performance IX, pp. 47–61 (1981)
8. Brandt, T., Dichgans, J., Koenig, E.: Differential effects of central versus peripheral vision on egocentric and exocentric motion perception. Exp. Brain Res. **16**(5), 476–491 (1973). https://doi.org/10.1007/BF00234474
9. Chelen, W., Kabrisky, M., Rogers, S.: Spectral analysis of the electroencephalographic response to motion sickness. Aviat. Space Environ. Med. **64**(1), 24–29 (1993)
10. Cheung, B., Hofer, K., Heskin, R., Smith, A.: Physiological and behavioral responses to an exposure of pitch illusion in the simulator. Aviat. Space Environ. Med. **75**(8), 657–665 (2004)
11. Cheung, B., Howard, I., Nedzelski, J., Landolt, J.: Circularvection about earth-horizontal axes in bilateral labyrinthine-defective subjects. Acta oto-laryngologica **108**(5–6), 336–344 (1989)
12. Dennison, M.S., Wisti, A.Z., D'Zmura, M.: Use of physiological signals to predict cybersickness. Displays **44**, 42–52 (2016)
13. Deutschländer, A., Bense, S., Stephan, T., Schwaiger, M., Dieterich, M., Brandt, T.: Rollvection versus linearvection: comparison of brain activations in pet. Human Brain Mapp. **21**(3), 143–153 (2004)
14. Dichgans, J., Brandt, T.: Visual-vestibular interaction: effects on self-motion perception and postural control. In: Held, R., Leibowitz, H.W., Teuber, H.L. (eds.) Perception, pp. 755–804. Springer, Heidelberg (1978). https://doi.org/10.1007/978-3-642-46354-9_25
15. Ebenholtz, S.M.: Motion sickness and oculomotor systems in virtual environments. Pres. Teleoper. Virtual Environ. **1**(3), 302–305 (1992)

16. Ebenholtz, S.M., Cohen, M.M., Linder, B.J.: The possible role of nystagmus in motion sickness: a hypothesis. Aviat. Space Environ. Med. **65**(11), 1032–1035 (1994)
17. Ehrlich, J.A., Kolasinski, E.M.: A comparison of sickness symptoms between dropout and finishing participants in virtual environment studies. In: Proceedings of the Human Factors and Ergonomics Society Annual Meeting, vol. 42, pp. 1466–1470. SAGE Publications, Los Angeles (1998)
18. Fauville, G., Queiroz, A., Woolsey, E.S., Kelly, J.W., Bailenson, J.N.: The effect of water immersion on vection in virtual reality. Sci. Rep. **11**(1), 1–13 (2021)
19. Fetter, M.: Vestibulo-ocular reflex. Neuro-Ophthalmol. **40**, 35–51 (2007)
20. Fischer, M., Kornmüller, A.: Optokinetisch ausgelöste bewegungswahrnehmungen und optokinetischer nystagmus [perception of motion based on the optokinetic sense and optokinetic nystagmus]. J. für Psychologie und Neurologie **41**, 273–308 (1930)
21. Guo, C., So, R.: Effects of foveal retinal slip on visually induced motion sickness: a pilot study. In: Proceedings of the Human Factors and Ergonomics Society Annual Meeting, vol. 56, pp. 2565–2569. SAGE Publications, Los Angeles (2012)
22. Himi, N., Koga, T., Nakamura, E., Kobashi, M., Yamane, M., Tsujioka, K.: Differences in autonomic responses between subjects with and without nausea while watching an irregularly oscillating video. Auton. Neurosci. **116**(1–2), 46–53 (2004)
23. Holmes, S.R., Griffin, M.J.: Correlation between heart rate and the severity of motion sickness caused by optokinetic stimulation. J. Psychophysiol. **15**(1), 35 (2001)
24. Hu, S., Grant, W.F., Stern, R.M., Koch, K.L.: Motion sickness severity and physiological correlates during repeated exposures to a rotating optokinetic drum. Aviat. Space Environ. Med. **62**, 308–314 (1991)
25. Jaekl, P., Jenkin, M., Harris, L.R.: Perceiving a stable world during active rotational and translational head movements. Exp. Brain Res. **163**(3), 388–399 (2005)
26. Jäger, M., Gruber, N., Müri, R., Mosimann, U.P., Nef, T.: Manipulations to reduce simulator-related transient adverse health effects during simulated driving. Med. Biol. Engi. Comput. **52**(7), 601–610 (2014)
27. Jarmasz, J., Hollands, J.G.: Confidence intervals in repeated-measures designs: the number of observations principle. Can. J. Exp. Psychol./Revue canadienne de psychologie expérimentale **63**(2), 124 (2009)
28. Ji, J.T., So, R.H., Cheung, R.T.: Isolating the effects of vection and optokinetic nystagmus on optokinetic rotation-induced motion sickness. Human Fact. **51**(5), 739–751 (2009)
29. Jongkees, L.: Physiologie und pathophysiologie des vestibularorganes. Archiv für klinische und experimentelle Ohren-, Nasen-und Kehlkopfheilkunde **194**(1), 1–110 (1969)
30. Kennedy, R.S., Stanney, K.M.: Postural instability induced by virtual reality exposure: development of a certification protocol. Int. J. Human-Comput. Interact. **8**(1), 25–47 (1996)
31. Keshavarz, B., Berti, S.: Integration of sensory information precedes the sensation of vection: a combined behavioral and event-related brain potential (erp) study. Behav. Brain Res. **259**, 131–136 (2014)
32. Keshavarz, B., Campos, J.L., Berti, S.: Vection lies in the brain of the beholder: EEG parameters as an objective measurement of vection. Front. Psychol. **6**, 1581 (2015)

33. Keshavarz, B., Hettinger, L.J., Vena, D., Campos, J.L.: Combined effects of auditory and visual cues on the perception of vection. Exp. Brain Res. **232**(3), 827–836 (2013). https://doi.org/10.1007/s00221-013-3793-9
34. Kim, J., Palmisano, S.: Eccentric gaze dynamics enhance vection in depth. J. Vision **10**(12), 7 (2010)
35. Kim, Y.Y., Kim, H.J., Kim, E.N., Ko, H.D., Kim, H.T.: Characteristic changes in the physiological components of cybersickness. Psychophysiology **42**(5), 616–625 (2005)
36. Kirollos, R., Allison, R.S., Palmisano, S.: Cortical correlates of the simulated viewpoint oscillation advantage for vection. Multisensory Res. **30**(7–8), 739–761 (2017)
37. Kirollos, R., Herdman, C.M.: Measuring circular vection speed in a virtual reality headset. Displays **69**, 102049 (2021)
38. Koohestani, A., et al.: A knowledge discovery in motion sickness: a comprehensive literature review. IEEE Access **7**, 85755–85770 (2019)
39. Kothgassner, O.D.: Salivary cortisol and cardiovascular reactivity to a public speaking task in a virtual and real-life environment. Comput. Human Behav. **62**, 124–135 (2016)
40. LaViola Jr., J.J.: A discussion of cybersickness in virtual environments. ACM Sigchi Bull. **32**(1), 47–56 (2000)
41. Melcher, G.A., Henn, V.: The latency of circular vection during different accelerations of the optokinetic stimulus. Percept. Psychophys. **30**(6), 552–556 (1981)
42. Nilsson, N.C., Nordahl, R., Sikström, E., Turchet, L., Serafin, S.: Haptically induced illusory self-motion and the influence of context of motion. In: Isokoski, P., Springare, J. (eds.) EuroHaptics 2012. LNCS, vol. 7282, pp. 349–360. Springer, Heidelberg (2012). https://doi.org/10.1007/978-3-642-31401-8_32
43. Owens, D.A., Gu, J., McNally, R.D.: Perception of the speed of self-motion vs. object-motion: another example of two modes of vision? Conscious. Cogn. **64**, 61–71 (2018)
44. Palmisano, S., Allison, R.S., Schira, M.M., Barry, R.J.: Future challenges for vection research: definitions, functional significance, measures, and neural bases. Front. Psychol. **6**, 193 (2015)
45. Palmisano, S., Barry, R.J., De Blasio, F.M., Fogarty, J.S.: Identifying objective EEG based markers of linear vection in depth. Front. Psychol. **7**, 1205 (2016)
46. Palmisano, S., Burke, D., Allison, R.S.: Coherent perspective jitter induces visual illusions of self-motion. Perception **32**(1), 97–110 (2003)
47. Palmisano, S., Gillam, B.: Stimulus eccentricity and spatial frequency interact to determine circular vection. Perception **27**(9), 1067–1077 (1998)
48. Reason, J.T.: Motion sickness adaptation: a neural mismatch model. J. Royal Soc. Med. **71**(11), 819–829 (1978)
49. Reason, J.T., Brand, J.J.: Motion Sickness. Academic press, Cambridge (1975)
50. Rebenitsch, L., Owen, C.: Review on cybersickness in applications and visual displays. Virtual Reality **20**(2), 101–125 (2016). https://doi.org/10.1007/s10055-016-0285-9
51. Riccio, G.E., Stoffregen, T.A.: An ecological theory of motion sickness and postural instability. Ecol. Psychol. **3**(3), 195–240 (1991)
52. Riecke, B.E., Feuereissen, D., Rieser, J.J., McNamara, T.P.: Spatialized sound enhances biomechanically-induced self-motion illusion (vection). In: Proceedings of the SIGCHI Conference on Human Factors in Computing Systems, pp. 2799–2802 (2011)
53. St George, R.J., Day, B.L., Fitzpatrick, R.C.: Adaptation of vestibular signals for self-motion perception. J. Physiol. **589**(4), 843–853 (2011)

54. Stephan, T.: Functional MRI of galvanic vestibular stimulation with alternating currents at different frequencies. Neuroimage **26**(3), 721–732 (2005)
55. Stern, R., Koch, K., Leibowitz, H., Lindblad, I., Shupert, C., Stewart, W.: Tachygastria and motion sickness. Aviat. Space Environ. Med. **56**(11), 1074–1077 (1985)
56. Stern, R.M., Koch, K.L., Stewart, W.R., Lindblad, I.M.: Spectral analysis of tachygastria recorded during motion sickness. Gastroenterology **92**(1), 92–97 (1987)
57. Strychacz, C., Viirre, E., Wing, S.: The use of EEG to measure cerebral changes during computer-based motion-sickness-inducing tasks. In: Biomonitoring for Physiological and Cognitive Performance during Military Operations, vol. 5797, pp. 139–148. International Society for Optics and Photonics (2005)
58. Tokumaru, O., Kaida, K., Ashida, H., Yoneda, I., Tatsuno, J.: EEG topographical analysis of spatial disorientation. Aviat. Space Environ. Medicine **70**(3 Pt 1), 256–263 (1999)
59. Wan, H., Hu, S., Wang, J.: Correlation of phasic and tonic skin-conductance responses with severity of motion sickness induced by viewing an optokinetic rotating drum. Percept. Motor Skills **97**(3_suppl), 1051–1057 (2003)
60. Watson, G.: A synthesis of simulator sickness studies conducted in a high-fidelity driving simulator. In: Proceedings of Driving Simulation Conference, pp. 69–78 (2000)
61. Webb, N.A., Griffin, M.J.: Optokinetic stimuli: motion sickness, visual acuity and eye movements. Aviat. Space Environ. Med. **73**(4), 351–358 (2002)
62. Wibirama, S., Hamamoto, K.: Investigation of visually induced motion sickness in dynamic 3d contents based on subjective judgment, heart rate variability, and depth gaze behavior. In: 2014 36th Annual International Conference of the IEEE Engineering in Medicine and Biology Society, pp. 4803–4806. IEEE (2014)
63. Wiest, G., Amorim, M.A., Mayer, D., Schick, S., Deecke, L., Lang, W.: Cortical responses to object-motion and visually-induced self-motion perception. Cogn. Brain Res. **12**(1), 167–170 (2001)
64. Wright, W., DiZio, P., Lackner, J.: Vertical linear self-motion perception during visual and inertial motion: more than weighted summation of sensory inputs. J. Vestib. Res. **15**(4), 185–195 (2005)
65. Wu, J.P.: EEG changes in man during motion sickness induced by parallel swing. Space Med. Med. Eng. **5**(3), 200–205 (1992)
66. Yang, X., Wang, D., Hu, H., Yue, K.: P-31: visual fatigue assessment and modeling based on ECG and EOG caused by 2D and 3D displays. In: SID Symposium Digest of Technical Papers, vol. 47, pp. 1237–1240. Wiley Online Library (2016)
67. Yang, J., Guo, C., So, R., Cheung, R.: Effects of eye fixation on visually induced motion sickness: are they caused by changes in retinal slip velocity? In: Proceedings of the Human Factors and Ergonomics Society Annual Meeting. vol. 55, pp. 1220–1224. SAGE Publications Sage CA, Los Angeles (2011)